Available online at www.sciencedirect.com
SCIENCE DIRECT
Vaccine 24 (2006) 5655–5669
Vaccine
www.elsevier.com/locate/vaccine

DNA prime and protein boost immunization with innovative polymeric cationic core-shell nanoparticles elicits broad immune responses and strongly enhance cellular responses of HIV-1 *tat* DNA vaccination

Arianna Castaldello [a,1], Egidio Brocca-Cofano [a,1], Rebecca Voltan [a], Chiara Triulzi [a], Giuseppe Altavilla [c], Michele Laus [d], Katia Sparnacci [d], Marco Ballestri [e], Luisa Tondelli [e], Cinzia Fortini [b], Riccardo Gavioli [b], Barbara Ensoli [f], Antonella Caputo [a,*]

[a] *Department of Histology, Microbiology and Medical Biotechnology, Section of Microbiology, University of Padova, Via A. Gabelli 63, 35122 Padova, Italy*
[b] *Department of Biochemistry and Molecular Biology, University of Ferrara, Ferrara, Italy*
[c] *Department of Pathological Anatomy and Histology, University of Padova, Padova, Italy*
[d] *Department of Life and Ambient Sciences, University of Piemonte Orientale and INSTM, UdR, Alessandria, Italy*
[e] *I.S.O.F., Consiglio Nazionale delle Ricerche, Bologna, Italy*
[f] *National AIDS Center, Istituto Superiore di Sanità, Roma, Italy*

Received 22 December 2005; received in revised form 10 May 2006; accepted 16 May 2006
Available online 2 June 2006

Abstract

Novel biocompatible core-shell cationic nanoparticles, composed of an inner hard core of poly(methylmethacrylate) (PMMA) and a hydrophilic tentacular shell bearing positively charged groups and poly(ethyleneglycol) chains covalently bound to the core, were prepared by emulsion polymerization and characterized in vitro and in vivo for DNA vaccine applications. The nanoparticles reversibly adsorbed large amounts of DNA, mainly through electrostatic interactions, preserved its functional structure, efficiently delivered it intracellularly, and were not toxic in vitro or in mice. Furthermore, two intramuscular (i.m.) immunizations (4 weeks apart) with a very low dose (1 μg) of the plasmid pCV-*tat* delivered by these nanoparticles followed by one or two protein boosts induced significant antigen-specific humoral and cellular responses and greatly increased Th1-type T cell responses and CTLs against HIV-1 Tat.

Keywords: Biocompatible nanoparticles; HIV-1 *tat*; DNA vaccination; Cellular responses

1. Introduction

Genetic vaccination using plasmid DNA represents an unique opportunity for achieving potent immune responses without the potential limitations of conventional live attenuated vaccines. These include the risk of reversion to a virulent state, restricted cell targeting, limited DNA carrying capacity, limitation by pre-existing immune responses, production and packaging problems and high production costs as well as various regulatory issues regarding approval for human use. Naked DNA-based vaccines have been shown to induce long-lived humoral and cellular immune responses both in experimental systems and in humans and protective immunity in animal challenging models [1,2]. However, multiple immunizations of high doses of DNA (100 μg in mice and up to 2–4 mg in non-human primates or in humans) are generally required to elicit effective immune responses [3,4]. It is likely that the high doses and multiple boosts required are due to massive enzymatic degradation, both extra- and intracellularly, of the majority of the DNA molecules injected,

* Corresponding author. Tel.: +39 049 8272350; fax: +39 049 8272355.
E-mail address: antonella.caputo@unipd.it (A. Caputo).
[1] A. Castaldello and E. Brocca-Cofano equally contributed to this study.

0264-410X/$ – see front matter © 2006 Elsevier Ltd. All rights reserved.
doi:10.1016/j.vaccine.2006.05.058

and to the poor efficiency of naked DNA transfection in vivo, so that few intact DNA molecules may be taken up by antigen presenting cells, reach the nucleus and be expressed and available for antigen presentation.

Several studies have already described the improvement of DNA vaccines using biological and synthetic adjuvants/delivery carriers, such as liposomes, immune-stimulating complexes, oil emulsions, cationic biopolymers, and biocompatible/biodegradable polymeric nano-and micro-particles [5–12]. The use of some microparticulate systems has been shown to protect DNA from degradation, to direct it efficiently to antigen-presenting cells, improving MHC class I and II molecules presentation and immune responses [13–19]. However, a serious limitation to the use of several new adjuvants/delivery systems in humans is often represented by their reactogenicity [12,20]. This renders the development of novel, safe and cost-effective delivery systems/adjuvants a crucial issue.

Biodegradable microparticles, produced with polymers such as poly(D,L-lactide) (PLA) and poly(D,L-lactide co-glycolide) (PLG), have been extensively used as delivery systems of entrapped drugs and antigens [9,21–26]. Encapsulated antigens are protected from unfavourable conditions (e.g. pH, bile salts and proteolytic enzymes) encountered after parenteral or mucosal administration [9,27]. However, encapsulation-based approaches are often associated with instability and degradation of the entrapped molecules occuring both during the encapsulation and release processes [28,29]. To overcome these problems, physical adsorption on the surface of nano- and micro-particles has very recently been proposed and shown to be a simpler, more efficient and less damaging procedure for the antigen [13,14,16–18,30–34]. The reversible adsorption of the antigen to the surface of the nano- and micro-particles has been achieved with the addition of surfactants and/or detergents during particle preparation. However, the use of such reagents often interferes with the reproducibility of particle size and size distribution, and of the vaccine formulation, and may affect the biocompatibility of the particles, thereby causing a possible impairment of their scaling up for future clinical development.

In the effort to develop improved DNA vaccine delivery systems, innovative polymeric nanoparticles able to bind DNA on their surface without the need for added surfactants and/or detergents were synthesized by emulsion polymerization and physico-chemically characterized. These novel particles exhibit a core-shell structure with an inner core constituted by poly(methylmethacrylate) (PMMA) and a highly hydrophilic outer shell, bearing poly(ethyleneglycol) chains and positively charged groups. PMMA is a highly biocompatible and slowly bioerodible polymer in the form of nanoparticles [35]. The poly(ethylenglycol) chains are able to prevent opsonization and the positive charges to reversibly associate with the DNA. The innovation in this technology is the presence of surface functional groups which are covalently bound to the core, and not simply adsorbed. The advantage of this strategy prevents physical desorption and/or instability/toxicity effects associated with vaccine formulations containing free surfactants and/or detergents, and ensures the generation of monodisperse, stable and reproducible particles and vaccine formulations. Since recent studies have shown that HIV-1 Tat (protein and DNA) represents a relevant antigen for the development of a prophylactic and/or therapeutic vaccine against AIDS (for review refer to [36,37]), the HIV-1 *tat* gene was selected as the model antigen to characterize these novel cationic nanoparticles. In particular, studies were addressed to investigate whether the particles were capable of reversibly adsorbing DNA, preserving its native conformation, biological activity, and shelf-life, and delivering/expressing it intracellularly. Finally, in view of their potential development as new delivery systems for DNA vaccine application, the safety and immunogenicity of vaccine formulations containing these nanoparticles were studied in Balb/c mice using a DNA prime-protein boost protocol and compared to immunization with naked *tat* DNA. The results indicated that these nanoparticles efficiently bind DNA molecules, mainly through electrostatic interactions, preserve DNA conformation and activity, deliver it into the cells in the absence of any in vitro or in vivo cytoxicity, increase the shelf-life of DNA, and enhance the antigen-specific cellular responses and CTLs even with the use of a very low dose of DNA and few immunizations.

2. Materials and methods

2.1. Synthesis

Nanoparticles (PEG32) were synthesized by emulsion polymerization [38]. Briefly, in a typical emulsion polymerization reaction, 500 ml of water containing 4.38 g of the ionic comonomer 1 [2-(dimethyloctyl)ammonium ethyl methacrylate bromine] and 4.5 g of the appropriate amount of non-ionic comonomer 2 [poly(ethylene glycol) (PEG) methyl ether methacrylate] (Fig. 1A) were introduced in a five-neck reactor equipped with mechanical stirring and reflux condenser, and heated at 80 °C under nitrogen atmosphere. Then, 25 ml of methyl methacrylate (monomer) were added. The system was let to stabilize for 30 min, and 250 mg of potassium persulfate (KPS) were added. The polymerization reaction was performed at 80 ± 1.0 °C for 2 h under constant stirring. At the end of the reaction, the product was purified by repeated dialysis [39], at least 10 times, against water to remove the residual monomer and comonomers. After this procedure, the polymeric nanoparticles were dried under vacuum at room temperature. A yield of 60%, with respect to the total amount of methyl methacrylate and of water-soluble comonomers, was obtained. 2-(Dimethylamino)ethyl methacrylate (DMAEMA), 1-bromo-octane and poly(ethylene glycol) methyl ether methacrylate (Mn = 2080) were purchased from Aldrich. KPS was pur-

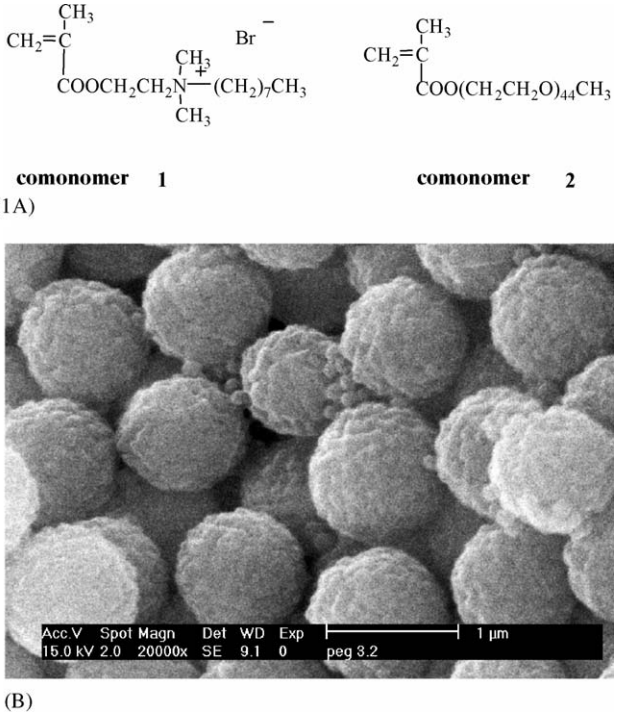

Fig. 1. (A) Ionic comonomer 1 [2-(dimethyloctyl)ammonium ethyl methacrylate bromine] and non-ionic comonomer 2 [poly(ethylene glycol) methyl ether methacrylate] used in the emulsion polymerization reaction. (B) SEM images of PEG32 core-shell nanoparticles.

chased from Carlo Erba. All these products were used without further purification. Methyl methacrylate (MMA) was purchased from Aldrich and distilled under vacuum just before use. The ionic comonomer 1 was obtained as previously reported [40]. A sample of yellow–green fluorescent nanoparticles (P-Fluo) was also synthetized using the same procedure as for PEG32 by adding a fluoresceine-allylic monomer to the reaction mixture [41].

2.2. Particle size, morphology and ξ-potential measurements

Particle size and size distribution were measured using a JEOL JSM-35CF scanning electron microscope (SEM) operating at an accelerating voltage of 15 kV. The samples were sputter coated under vacuum with a thin layer (10–30 Å) of gold. The SEM photograph were digitalizated and elaborated by the Scion Image processing program (Scion Corporation, www.scioncorp.com). From 200 to 250 individual microsphere diameters were measured for each sample to determine the number-average diameter $\bar{D}_n$[42], the weight-average diameter $\bar{D}_w$[42], and the uniformity ratio U [42]. The average particle size and polydispersity index (PI) were determined by dynamic light scattering (DLS) at 25 °C by a Zetasizer 3000 HS system (Malvern, UK) using a 10 mV He–Ne laser. For data analysis, the viscosity and refractive indexes of pure water at 25 °C were used. The instrument was calibrated with standard polystyrene latex particles of 200 nm in diameter. To achieve a constant ionic background, the samples were diluted in 10 mM NaCl to a concentration of 20 μg/ml. Each value is the average of five measurements. The amount of quaternary ammonium groups per gram of nanoparticles was determined by potentiometric titration of the bromine ions obtained after complete ionic exchange. This was accomplished by dispersing in a beaker 0.5–1 g of each nanoparticle sample in 25 ml of 1 M KNO_3 at room temperature for 48 h. The mixture was then adjusted to pH 2 with H_2SO_4, and the bromine ions in solution were titered with 0.01 M $AgNO_3$. Nanoparticles were stored lyophilized at room temperature or in suspension (10 mg/ml) either at room temperature or at 4 °C.

2.3. Plasmids

Plasmid pCV-*tat*, expressing the HIV-1 *tat* cDNA (HLTV-III, BH10 clone) under the transcriptional control of the adenovirus major late promoter, plasmid pCV-0 [43], and plasmid pGL2-CMV-Luc-basic (Promega, WI, USA), expressing the luciferase gene, under the transcriptional control of the human cytomegalovirus promoter, were purified using the Plasmid Maxi kit provided by Qiagen (Hilden, Germany), according to the manufacturer's instructions, and resuspended in sterile phosphate-buffered saline (PBS), without calcium and magnesium.

2.4. Cell-free adsorption/release experiments

Freeze-dried nanoparticles (5 mg) were suspended in 20 mM or in 150 mM (commercial PBS) sodium phosphate buffers (pH 7.4) in a volume of 500 μl, and stirred for 5 min. Increasing amounts of plasmid DNA (0–250 μg/ml) were then added. The suspensions were continuously stirred for 2 h at room temperature. After microfuge centrifugation at 9000 rpm for 15 min, the supernatant was collected, filtered through a Millex GV_4 filter unit (0.22 μm, Millipore, Milan, Italy), and UV absorbance at 260 nm was measured to determine the amount of unbound DNA. Adsorption efficiency (%) was calculated as 100 × [(administered DNA) − (unbound DNA)/(administered DNA)]. The experiment was repeated three times (S.D. ≤ 6%). For DNA release experiments, DNA/PEG32 complexes were prepared using 400 μg of DNA/10 mg of PEG32/ml of phosphate buffer (pH 7.4). After 2 h incubation at room temperature, the complexes were collected by centrifugation, washed twice with water, resuspended in PBS (pH 7.4) (same volume used for complex assembly) containing increasing concentration of NaCl (up to 1 M), and incubated at 37 °C under continuous stirring. At different time intervals, samples were spun at 9000 rpm for 15 min and the amount of desorbed DNA determined by UV spectroscopy at 260 nm. Release efficiency (%) was determined as 100× (released DNA/bound DNA). The experiment was repeated three times (S.D. ≤ 7%). In some experi-

ments, the desorbed DNA was also visualized by agarose gel electrophoresis.

2.5. Preparation of DNA/nanoparticle complexes

For in vitro cell culture experiments and in vivo studies, complexes were prepared in 20 mM sodium phosphate buffer (pH 7.4) by mixing 10 μg of DNA/1 mg of PEG32/100 μl of buffer (in vitro studies) or 1 μg of DNA/1 mg of PEG32/100 μl (in vivo studies) under continuous stirring for 2 h at room temperature. The complexes were collected by microfuge centrifugation at 9000 rpm for 15 min, resuspended in the appropriate volume of 20 mM sodium phosphate buffer (pH 7.4) and used immediately (fresh). To evaluate the stability of the complexes, in some experiments DNA/PEG32 pellets were resuspended in 20 mM phosphate buffer, lyophilized (Modulajo Edwards, Crawley, Sussex, GB) and stored at room temperature until use. Immediately before use, they were hydrated for 1 h at room temperature in the appropriate volume of 20 mM sodium phosphate buffer (pH 7.4).

2.6. Cell cultures

Monolayer cultures of HeLa and HL3T1 cells were grown in DMEM (Gibco, Grand Island, NY, USA) containing 10% heat-inactivated FBS (Hyclone, Logan, UT). HL3T1 cells are HeLa cells containing an integrated copy of the bacterial chloramphenicol acetyl transferase (CAT) reporter gene under the transcriptional control of the HIV-1 LTR promoter [44]. BALB/c 3T3-Tat murine fibroblasts (aplotype H^{2kd}), stably transfected with plasmid pRP-neo-Tat, were described previously [45] and grown in DMEM supplemented with 10% FBS. P815 cells (aplotype H^{2kd}) derived from a murine mastocytome were obtained through ATCC and grown in DMEM containing 10% FBS.

2.7. Analysis of cytotoxicity in vitro

Cells (1×10^4/100 μl) were seeded in 96-well plates and cultured for 96 h at 37 °C with increasing concentrations of sample PEG32 (0.05–10 mg/ml) (sestuplicate wells). Cell proliferation was measured using the colorimetric cell proliferation kit I (MTT based) (Roche, Milan, Italy) [46] and compared to that of untreated cells. The experiment was repeated three times (S.D. ≤ 13%).

2.8. Cellular uptake

Cellular uptake of the DNA/nanoparticle complexes was evaluated with a fluorescent nanoparticle sample (P-Fluo). Cells (5×10^4/well) were seeded in 24-well plates containing 12-mm coverslips and cultured at 37 °C. Twenty-four hours later, DNA/P-fluo complexes were added to the cells, in 200 μl of DMEM containing 10% FBS. Cells samples were also incubated with P-fluo unloaded nanoparticles. Controls were represented by untreated cells. At different time intervals, cells were washed with PBS, fixed with 4% cold paraformaldehyde and observed at a confocal laser scanning microscope LSM410 (Zeiss, Oberkochen, Germany). Image acquisition, recording and filtering were carried out using a Indy 4400 graphic workstation (Silicon Graphics, Mountain View, CA, USA) as previously described [47].

2.9. Evaluation of gene expression in vitro

Uptake, release and gene expression of DNA/PEG32 formulations was evaluated in HeLa cells using 10 μg of a reporter plasmid DNA (pGL2-CMV-Luc-basic)/mg of particles. Cells (5×10^5) were seeded in 60-mm Petri dishes, cultured at 37 °C for 24 h and incubated with the DNA/nanoparticle complexes. Controls were cells incubated with the naked DNA (10 μg), and untreated cells. Forty-eight hours later the activity of the reporter gene was measured on amounts of cell extracts normalized to the total protein contents, using the Luciferase Assay Systems (E1500, Promega), according to the manufacturer's instructions. Experiments were run in duplicate.

2.10. Mice immunization

Seven-weeks-old female BALB/c (H^{2kd}) mice (Harlan, Udine, Italy) were immunized with plasmid pCV-*tat* (1 μg), alone or complexed with PEG32 (1 mg), in a final volume of 100 μl. Controls were injected with plasmid pCV-0 (1 μg) alone or associated to the nanoparticles. Each experimental group was composed of 14 mice. Animals were immunized with the DNA/nanoparticle complexes or with naked DNA at weeks 0 and 4, and boosted with Tat protein (1 μg) in Alum, or with Alum alone (controls), at weeks 8 (two DNA primes-one protein boost regimen) and 12 (two DNA primes-two protein boosts regimen) after the first immunization. Immunogens were given to each mouse by bilateral intramuscular (i.m.) injections in the quadriceps muscles of the posterior legs (50 μl/leg). During the course of the experiments, animals were controlled twice a week at the site of injection and for their general conditions (such as liveliness, food intake, vitality, weight, motility, sheen of hair). Mice were sacrificed at week 10 ($n = 3$) (for the two DNA primes-one protein boost regimen), and at weeks 14 ($n = 3$) and 29 ($n = 8$) (for the two DNA primes-two protein boosts regimen), to collect blood and organs for analysis of humoral and cellular responses, and for histological, histochemical and immunohistochemical studies. The experiment was repeated three times.

2.11. Tat protein and peptides

The 86-aa long Tat protein (HTLVIIIB, BH-10 clone) was expressed in *Escherichia coli*, as previously described [48–50], and provided by Diatheva (Fano, Italy). The puri-

fied Tat protein is >95% pure as tested by SDS-PAGE, and HPLC analysis. To prevent oxidation that occurs easily because Tat contains seven cysteines, the Tat protein was stored lyophilized at −80 °C and resuspended in degassed sterile PBS (2 mg/ml) immediately before use [48–50]. In addition, since Tat is photo- and thermo-sensitive, the handling of Tat was always performed in the dark and on ice. The VCF (VCFITKALGISYGRK) Tat peptide containing a K^d-restricted CTL epitope and a CD4 T cell epitope (Caputo and Gavioli, unpublished data; [51]) was synthesized by UFPeptides s.r.l. (Ferrara, Italy). Peptide stocks were prepared in DMSO at 10^{-2} M concentration, kept at −80 °C, and diluted in PBS (for ELISA tests) or RPMI 1640 (for Elispot assays) before use.

2.12. Serology

Serological response against Tat (IgG titers, IgG1 and IgG2a isotypes, and IgG epitope mapping) was measured by enzyme-linked immunosorbent assay (ELISA) using 96-well immunoplates (Nunc-immunoplate F96 PolySorb) coated with 100 μl/well of Tat protein (1 μg/ml in 0.05 M carbonate buffer pH 9.6–9.8) for 12 h at 4 °C, or with Tat peptides (10 μg/ml in PBS containing BSA) for 2 h at 37 °C, as previously described [47].

2.13. Splenocytes purification

Splenocytes were purified from spleens squeezed on filters (Cell Strainer, 70 μm, Nylon, Becton Dickinson). Following red blood cell lysis with RBC lysing buffer (Sigma), cells were washed with RPMI 1640 containing 10% FBS (Hyclone), spun for 10 min at 1200 rpm, resuspended in RPMI 1640 containing 10% FBS and used for the analysis of cellular immune responses. Pool of spleens per experimental group were used. Depletion of B lymphocytes and purification of CD8+ T cells were carried out using anti-CD19 and anti-CD8 magnetic beads (BD Pharmingen, San Jose, CA, USA), according to the manufacturer's instructions. Cell cultures were then analyzed by fluorescence-activated cell sorter (FACSCalibur, BD) analysis using rat anti-mouse monoclonal antibodies (α-CD19, α-CD3, α-CD4, α-CD8) and a goat anti-rat FITC-conjugated antibody (all from BD Pharmingen).

2.14. Tat-specific T cell proliferation

Splenocytes (4×10^5/200 μl) were cultured in 96-well plates (sestuplicate wells) in the presence or absence of affinity-purified and biologically active Tat protein (0.1, 1, or 5 μg/ml) or Concanavaline A (2 μg/ml, Roche, Mannheim, Germany) for 5 days at 37 °C. [*methyl*-^{3}H]-Thymidine (2.0 Ci/mmol, NEN-DuPont) was added to each well (0.5 μCi), and cells were incubated for 16 h at 37 °C. [^{3}H]-Thymidine incorporation was measured with a β-counter (Top Count, Packard). The stimulation index (S.I.) was calculated by dividing the mean counts/min of six wells of antigen-stimulated cells by the mean counts/min of the same cells grown in the absence of the antigen.

2.15. CTL assays

Splenocytes were depleted of B cells and co-cultivated with Balb/Tat cells (ratio 5:1), previously irradiated with 30 Gy (^{137}Cs). After 3 days of culture, rIL-2 (10 U/ml) (Roche) was added and cells co-cultivated for additional 3 days at 37 °C. Dead cells were removed by Ficol gradient (Histopaque, Sigma). CTL activity was determined, at various effector/target ratios, by standard ^{51}Cr release assays using syngeneic P815 target cells, labeled with ^{51}Cr (25 μCi/3×10^6 cells; NEN, Du-Pont) for 90 min at 37 °C, and pulsed with the VCF Tat peptide (1×10^{-5} M), for 1 h at 37 °C. After 5 h incubation at 37 °C, the percentage of ^{51}Cr released was determined in the medium. Percent (%) of specific lysis was calculated as 100 × (cpm sample − cpm medium)/(cpm Triton-X100 − cpm medium). Spontaneous release was below 10% [52].

2.16. Enzyme-linked immunospot (Elispot) assays

Enzyme-linked immunospot assays were performed for Th1 (IFN-γ, IL-2) and Th2 (IL-4) cytokines, before and after in vitro restimulation, using commercially available murine IFN-γ, IL-2 and IL-4 Elispot kits (BD, Pharmingen), according to the manufacturer's instructions. Briefly, splenocytes (3×10^6/ml) were cultured with VCF Tat peptide (3 μg/ml) for 5 days and extensively washed with RPMI 1640 containing 10% FBS. Splenocytes, before stimulation (5×10^5 cells/well) or after peptide stimulation in vitro ($4–5 \times 10^4$ cells/well), were added to 96-well Elispot plates pre-coated with the cytokine-specific capture antibody, and incubated at 37 °C for 24 h in the absence (untreated) or presence of VCF Tat peptide (10^{-6} M) (duplicate wells). ConA (2 μg/ml) was used as a positive control for cytokine secretion. Spots were counted using an automated Elispot reader (AELVis 4.0, Hannover, Germany). The number of spots counted in the peptide-treated wells minus the number of spots counted in the untreated wells are the specific responses and they were considered significant when net spots/million cells were >20 (fresh) and >50 (after re-stimulation) and at least two times above the score of the untreated wells.

2.17. Histological, histochemical and immunohistochemical procedures

At sacrifice mice were subjected to autopsy. Sample of cutis, subcutis and skeletal muscles at the site of injection and other organs (lungs, heart, intestine, kidneys, spleen and liver) were taken and processed for histologic, histochemical and immunohistochemical examination, as described previously [47,53]. An average of 8–10 mice per experimental group was analysed.

2.18. Statistical analysis

Student's τ-test was performed as described [54].

3. Results

3.1. Synthesis and physico-chemical characterization of core-shell nanoparticles

Innovative biocompatible poly(methylmethacrylate) core-shell nanoparticles (diameter <1 μm) (Fig. 1) were produced by emulsion polymerization employing methyl methacrylate as the monomer, and two water-soluble comonomers, namely the non-ionic poly(ethylene glycol) methyl ether methacrylate (comonomer 2) able to stabilize the suspension and to provide a highly hydrated shell, and the ionic 2-(dimethyloctyl) ammonium ethyl methacrylate bromine (comonomer 1) bearing a positively charged quaternary ammonium group. The resulting nanoparticles are constituted by an inert polymeric core of PMMA surrounded by a highly hydrophilic outer shell bearing poly(ethylene glycol) chain brushes and cationic functional groups, able to reversibly associate with the DNA, covalently bound to the core. Sample PEG32 is characterized by an average SEM diameter of 960 ± 38 nm, and 18.0 μmol quaternary ammonium groups per gram of nanoparticles, as determined by potentiometric titration of the bromine ions following complete ionic exchange with KNO_3. Analysis of the ζ-potential (+32.2 ± 0.6 mV) confirmed that the cationic comonomer employed in the polymerization reaction is covalently bound to the nanoparticle surface. The nanoparticles were stored lyophilized at room temperature or in suspension either at room temperature or at 4 °C and under these conditions they were stable up to 5 years.

3.2. DNA adsorption and release

The capability of the core-shell nanoparticles to adsorb and release plasmid DNA molecules was evaluated in cell-free experiments. DNA binding experiments were run in 20 and 150 mM phosphate buffers (pH 7.4) at room temperature, as described in Section 2. As shown in Fig. 2A, the binding capacity of sample PEG32 was very high at low DNA concentration, and gradually decreased when the DNA concentration exceeded 50 μg/ml. Surface saturation occured when higher plasmid concentrations were used, showing a maximum loading value of 7.58 and 8.0 μg/mg of adsorbed DNA, respectively, in the presence of medium and low ionic strength buffers (20 and 150 mM phosphate buffers, pH 7.4). In contrast, binding did not occur when a high salt concentration (1 M NaCl) was used and, furthermore, no significant differences in binding ability were observed in the presence of isotonic buffers at pH 5.0 and 8.5 (data not shown). These results suggest that the adsorption mechanism is mainly driven by electrostatic interactions between negatively charged plas-

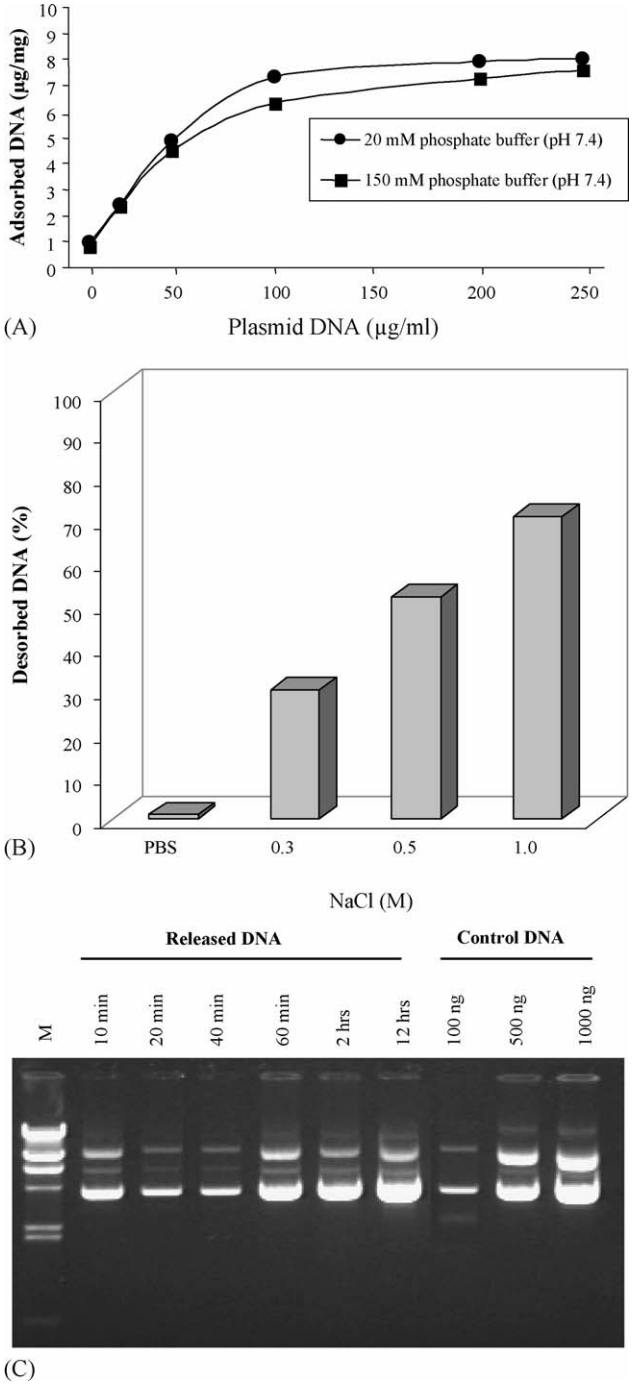

Fig. 2. Analysis of DNA binding and release. (A) DNA binding experiments were run in 20 and 150 mM phosphate buffers (pH 7.4) at room temperature, using 10 mg/ml of nanoparticles and increasing amounts of pCV-0 plasmid DNA (0–250 μg/ml). (B) DNA desorption experiments from PEG32 nanoparticles (80 μg DNA/10 mg/ml) were carried out at 37 °C in PBS (pH 7.4) and increasing amounts of NaCl. (C) pCV-0/PEG32 (100 μg DNA/10 mg/ml) complexes were incubated at 37 °C in the presence of 20 mM phosphate buffer (pH 7.4) containing 1 M NaCl. After incubation for different time periods, samples were centrifuged and the DNA released from the complexes was analyzed by agarose gel electrophoresis. The results of one representative experiment are shown. *M*, λ *Hin*dIII DNA molecular weight marker (1 μg); control DNA, 100, 500 and 1000 ng of pCV-0 plasmid DNA.

mid DNA molecules and positively charged groups on the nanoparticle surface.

Next, to assess the capacity of the nanoparticles to release the adsorbed DNA, several samples of DNA/PEG32 complexes were prepared with comparable amounts of loaded DNA (8 μg/mg) and incubated for 2 h at 37 °C in the presence of increasing concentrations of NaCl phosphate buffer (pH 7.4). Samples were centrifuged and the amount of DNA released from the complexes in supernatants was determined by means of UV spectrophotometry. As shown in Fig. 2B, an increase in the buffer's ionic strength induced a significant release of DNA from PEG32 (up to 80% in the presence of 1 M NaCl), further implying that ionic interactions represent the major driving force for DNA adsorption on these core-shell nanoparticles. Finally, in some experiments DNA/PEG32 complexes were incubated in the presence of phosphate buffer (pH 7.4) containing 1 M NaCl for several time intervals and the desorbed DNA was analyzed by agarose gel electrophoresis (Fig. 2C). These experiments showed that the DNA was promptly and continuously released from PEG32 preserving its structural integrity, for up to 12 h of incubation. Indeed, the ratio between super-coiled and coiled plasmid DNA configurations appeared unchanged, as compared to control plasmid DNA. As a whole, these results demonstrate that DNA is efficiently bound to and released from the particle surface and that is not degraded or damaged during the adsorption and release process.

3.3. Measurement of cytotoxicity in vitro

The cytotoxicity of sample PEG32 was assayed in HL3T1 cells following incubation with increasing amounts of nanoparticles. As shown in Fig. 3, no reduction ($p > 0.05$) in cell viability was observed up to 5 mg/ml of PEG32, as compared to untreated cells. Although a slight reduction (19%) of cell viability was observed at a very high dose of 10 mg/ml, the difference was not significant as compared to control cells

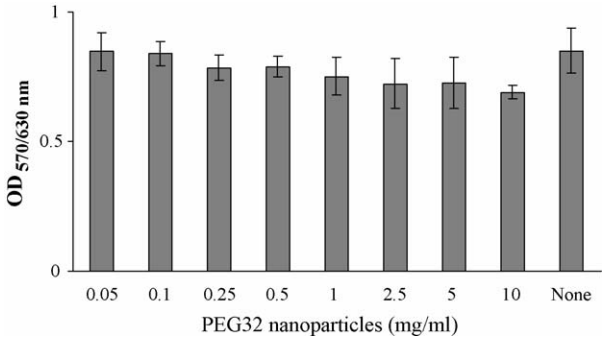

Fig. 3. Cell proliferation in the presence of PEG32 nanoparticles. HL3T1 cells were cultured for 96 h with increasing amounts of PEG32 (0.05–10 mg/ml), and cell proliferation was measured using a colorimetric MTT-based assay. Controls were represented by untreated cells (none). Results are expressed as the mean (±S.D.) of sextuples. The results of one representative experiment out of three are shown.

($p > 0.05$). These results indicate that the novel nanoparticles are not toxic for the cells.

3.4. Cellular uptake of nanoparticles

To evaluate cellular uptake, HL3T1 cells were cultured with a fluorescent nanoparticle sample (P-Fluo), which was synthesized in a fashion similar to PEG32 but with the addition of a small amount of fluoresceine-based allylic monomer in the reaction mixture. Cells were incubated for 24 h with P-fluo alone or complexed with pCV-0 plasmid DNA and analyzed under confocal microscopy. The detection of nanoparticles (Fig. 4A) and DNA/nanoparticle complexes (Fig. 4B) in the cytoplasm indicated that they were taken up by the cells in vitro.

3.5. Evaluation of gene expression

The capacity of the complexes to release intracellularly functional DNA was tested in HeLa cells using plasmid

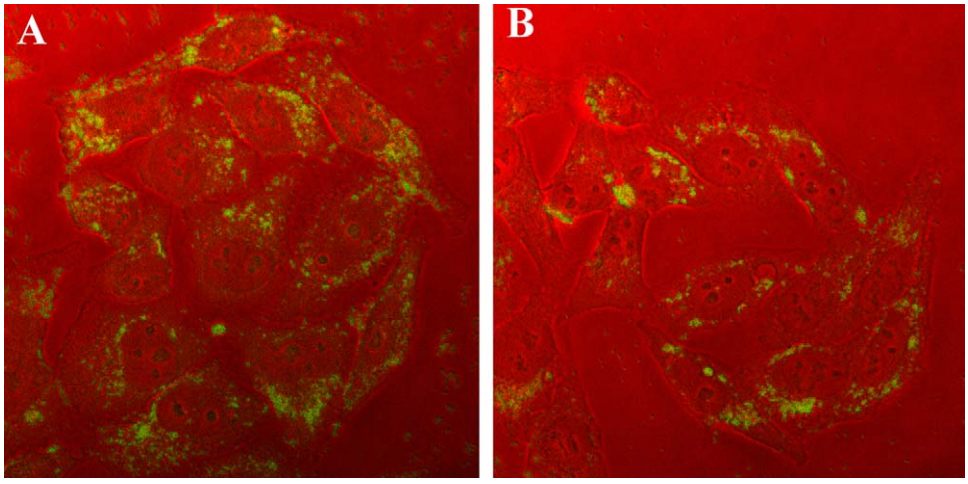

Fig. 4. Cellular uptake of P-fluo nanoparticles. HL3T1 cells were cultured in the presence of P-fluo nanoparticles (40 μg) alone (A) or associated with 1 μg of pCV-0 DNA (B). After 24 h of incubation, cells were fixed with paraformaldehyde and observed using confocal microscopy.

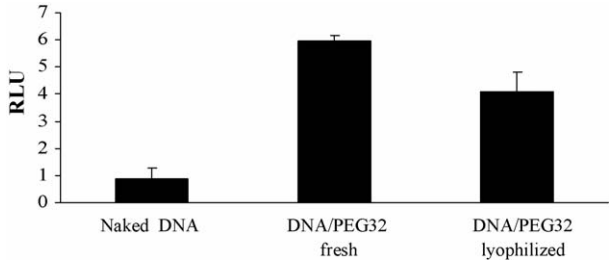

Fig. 5. Analysis of gene expression. HeLa cells were incubated with pGL2-CMV-Luc (10 μg) alone (naked DNA) or with freshly prepared DNA/PEG32 complexes (fresh). In addition, pGL2-CMV-Luc/PEG32 complexes were prepared, freeze-dried and stored at room temperature for 9 weeks. Lyophilized complexes were then resuspended and added to the cells (lyophilized). The results of one representative experiment out of three are shown.

pGL2-CMV-Luc (10 μg). Cells were incubated with freshly prepared pGL2-CMV-Luc/PEG32 complexes and expression of the luciferase reporter gene was compared to that observed in cells incubated with naked plasmid DNA. As shown in Fig. 5, luciferase gene expression was significantly higher ($p < 0.05$) in cells treated with the DNA/nanoparticle complexes (fresh) as compared to cells treated with the same dose of naked DNA where, in contrast, luciferase gene expression was barely detectable. These results indicate that PEG32 nanoparticles deliver, release and allow intracellular expression of the gene adsorbed on their surface. In addition, to evaluate the stability of the vaccine formulation, pGL2-CMV-Luc/PEG32 complexes were prepared, freeze-dried and stored at room temperature for 9 weeks. Lyophilized complexes were then hydrated in 20 mM sodium phosphate buffer (pH 7.4) and added to the cells. As shown in Fig. 5, expression of the luciferase gene was similar ($p > 0.05$) to that observed with the freshly prepared complexes, suggesting that the vaccine formulation is stable at room temperature.

3.6. Immunogenicity studies in mice

The immunogenic potential of novel DNA-based vaccines composed of PEG32 nanoparticles was studied in BALB/c mice. To this end, the HIV-1 *tat* gene was used as model antigen, since it is a vaccine relevant antigen and it has been already used in humans and in experimental animals.

Mice were immunized by the intramuscular route with a low amount of pCV-*tat* plasmid DNA (1 μg) adsorbed to PEG32. Control animals included mice injected with pCV-0 (1 μg)/PEG32 complexes. To compare the immune responses induced by this vaccine formulation to those induced by naked DNA, groups of mice received the pCV-*tat* plasmid DNA alone, or plasmid pCV-0 as control. In order to elicit antibody responses, which are known to be not induced or poorly induced by *tat* DNA vaccination, a DNA prime-protein boost regimen was used, as described in Section 2.

3.7. Analysis of Tat-specific cellular responses

Cell proliferation in response to the Tat protein was evaluated using the [^{3}H]-thymidine incorporation test on mice splenocytes cultured for 5 days in the presence of 0.1, 1 and 5 μg/ml of Tat. Antigen-specific and dose-dependent cell proliferation was detected in both groups of mice immunized with pCV-*tat*/PEG32 and pCV-*tat* alone (Fig. 6), but not in the untreated splenocytes nor in lymphocytes of control mice injected with pCV-0/PEG32 or pCV-0 alone. The proliferation index was generally higher in mice immunized with *tat*/PEG32, as compared to mice vaccinated with naked DNA.

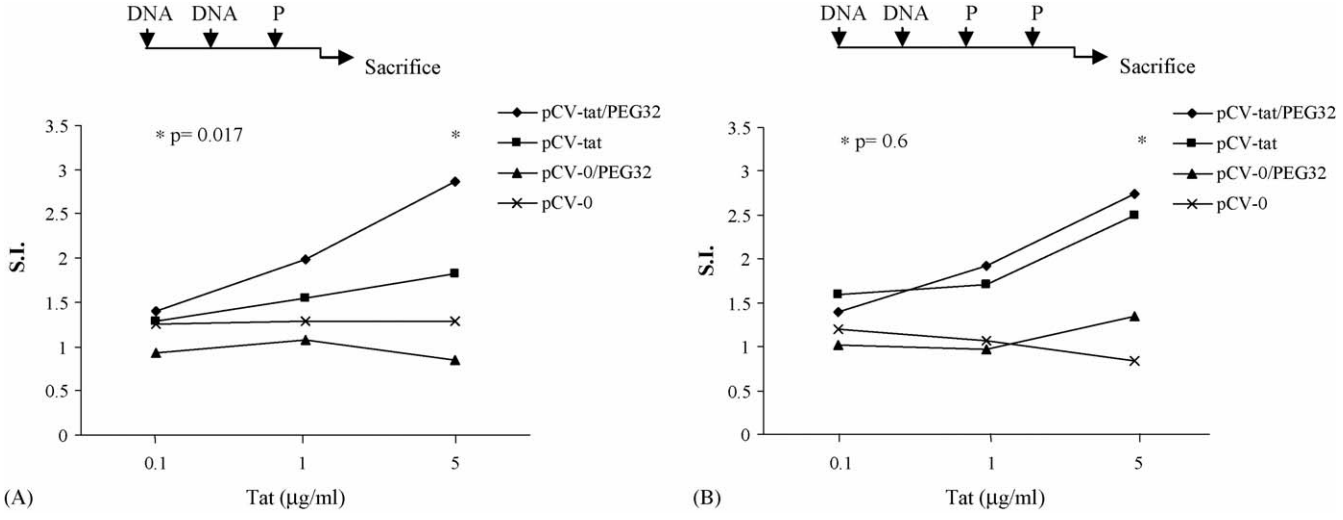

Fig. 6. Lymphoproliferation to Tat protein. Animals were primed with the DNA/nanoparticle complexes or with naked DNA at weeks 0 and 4, and boosted with the Tat protein (1 μg) in Alum, or with Alum alone (controls), at weeks 8 (two DNA prime-one protein boost regimen) and at week 12 (two DNA prime-two protein boosts regimen) after the first immunization. Mice were sacrificed at week 10 (for the two DNA prime-one protein boost regimen) (A), and at week 14 (B) (for the two DNA prime-two protein boosts regimen). Values represent the S.I. of murine splenocytes (pool of spleens) after Tat (0.1, 1 or 5 μg/ml) addition. The results of one representative experiment out of three are shown.

Of note, the difference was statistically significant only after one protein boost ($p = 0.017$) suggesting a considerable adjuvant effect of the nanoparticles.

To evaluate the nature of the cytokine profile generated by vaccination, splenocytes were also tested before and after peptide stimulation in vitro using the Elispot technique to evaluate production of IFN-γ (Th1-type response) and IL-4 (Th2-type response). In addition, production of IL-2 was tested to evaluate the capability of the vaccines to induce memory T cell responses. Immune responses were barely detectable before in vitro restimulation (data not shown) in agreement with the results of previous studies. However, antigen stimulation of splenocytes for 5 days enhanced these responses to a greater magnitude in both groups of vaccinated mice. After the two DNA primes-one protein boost regimen, the number of Tat-specific IFN-γ-secreting splenocytes was significantly higher in mice primed with *tat*/PEG32 as compared to mice primed with naked DNA ($p = 0.03$) (Fig. 7A). In addition, significant IL-4 ($p = 0.021$) and IL-2 ($p = 0.029$) responses were detected only after priming with the *tat*/PEG32 vaccine, whereas these responses were barely detectable in mice primed with naked DNA (Fig. 7A).

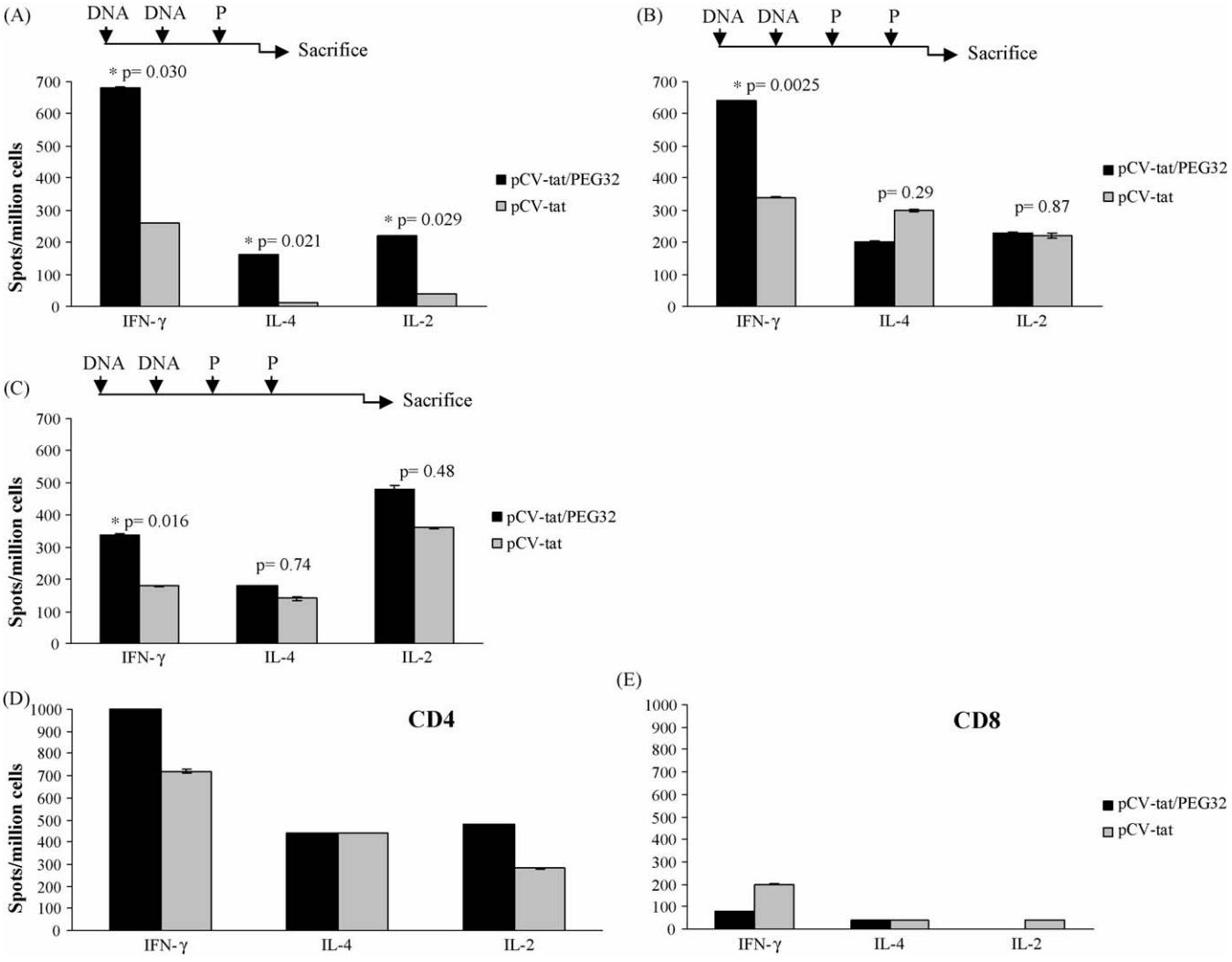

Fig. 7. Analysis of IFN-γ, IL-2 and IL-4 secretion by Elispot. Animals were immunized with the DNA/nanoparticle complexes or with naked DNA at weeks 0 and 4, and boosted with the Tat protein (1 μg) in Alum, or with Alum alone (controls), at weeks 8 (two DNA primes-one protein boost regimen) and 12 (two DNA primes-two protein boosts regimen) after the first immunization. Mice were sacrificed at week 10 (after the two DNA prime-one protein boost regimen) (A), and at weeks 14 ($n = 3$) (B) and 29 ($n = 8$) (C) (for the two DNA prime-two protein boosts regimen). (A, B, C) Spleens were pooled for each experimental group, stimulated in vitro for 5 days with a Tat 15-mer (VCF) peptide containing a CD4 and CD8 epitope, extensively washed, added to Elispot plates pre-coated with the cytokine-specific capture antibody, and incubated in the absence (untreated) or presence of the VCF peptide. (D, E) Animals were primed with the DNA/nanoparticle complexes or with naked DNA at weeks 0 and 4, and boosted at weeks 8 and at week 12 (two DNA prime-two protein boosts regimen) after the first immunization. Mice were sacrificed at week 29 ($n = 8$). After in vitro restimulation, cytokine production was determined on CD4-enriched (CD8-depleted) (D) and CD8-purified (E) T cell subpopulations. Specific responses corresponded to the number of spots counted in the peptide-treated wells minus the number of spots counted in the untreated wells. Responses were considered significant when net spots/million cells were >50 and at least two times above the score of the untreated wells. The results of one representative experiment out of three are shown.

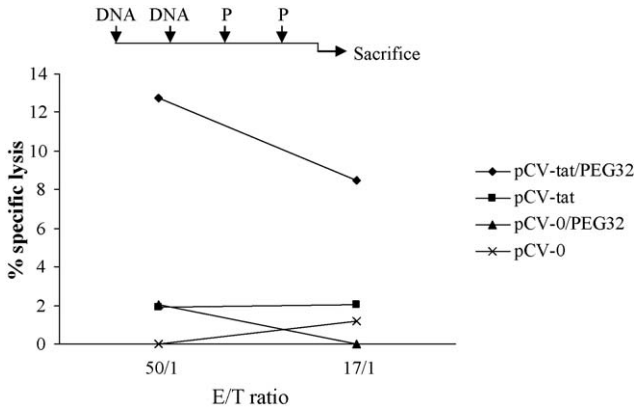

Fig. 8. CTL response to Tat. Animals were immunized with the DNA/nanoparticle complexes or with naked DNA at weeks 0 and 4, and boosted with the Tat protein (1 μg) in Alum, or with Alum alone (controls), at weeks 8 and 12 (two DNA primes-two protein boosts regimen) after the first immunization. Mice were sacrificed at week 14 after the first immunization. B-depleted splenocytes (pool of spleens) were co-cultivated with Balb/Tat cells and CTL activity was determined, at various effector/target (E/T) ratios, by standard ^{51}Cr release assays using syngenic P815 target cells pulsed with a VCF Tat peptide contaning a CTL epitope. The percentage (%) of specific lysis are reported.

After the two DNA primes-two protein boosts regimen, the number of Tat-specific IFN-γ-secreting cells was still significantly higher in *tat*/PEG32-primed mice ($p = 0.0025$), while antigen-specific IL-4 ($p = 0.29$) and IL-2 ($p = 0.87$) responses increased and reached comparable levels in mice primed with *tat*/PEG32 and with naked DNA (Fig. 7B).

Interestingly, the number of IFN-γ-secreting cells was significantly ($p < 0.05$) higher than the number of IL-4- and IL-2-secreting cells after two DNA primes-one protein boost, both in mice receiving the *tat*/PEG32 and in mice vaccinated with naked DNA (Fig. 7A). However, after the second protein boost, this difference was only significant ($p < 0.05$) in mice vaccinated with the *tat*/PEG32 vaccine. In fact, after the second protein boost, the numbers of IFN-γ-, IL-4- and IL-2-secreting cells were not statistically different ($p > 0.05$) in animals that were primed with naked DNA (Fig. 7B).

To assess whether IFN-γ responses were associated with cytotoxic function, B cell-depleted splenocytes were tested in ^{51}Cr-release assays after in vitro re-stimulation with syngeneic Tat-expressing cells. Specific anti-Tat CTLs capable of killing P815 target cells, pulsed with VCF Tat-derived peptide containing a Tat immunodominant CTL epitope, were detected only in mice primed with *tat*/PEG32 and boosted twice with Tat protein (Fig. 8). CTL responses were not detectable in mice receiving only one protein boost (data not shown).

Further, to assess whether the vaccines induced long-lasting cellular immunity, few mice receiving the two DNA primes-two protein boosts regimen were sacrificed 17 weeks after the second protein boost (week 29). As shown in Fig. 7C, IFN-γ-, IL-4- and IL-2-secreting cells were still detected at significant levels more than 4 months after the last immunization boost in both groups. Interestingly, while the number of IFN-γ-secreting cells decreased and IL-4 responses remained unchanged, IL-2 responses increased. Although the differences were not statistically significant ($p > 0.05$), higher IFN-γ, IL-4 and IL-2 responses persisted in mice primed with *tat*/PEG32.

Finally, to determine which T cell subset was the primary source of IFN-γ-, IL-4- and IL-2 secretion, mice were immunized with the two DNA primes-two protein boosts regimen and sacrificed 17 weeks after the second protein boost (week 29). Cytokine production was tested after in vitro restimulation on CD8+ purified and CD4+-enriched (CD8-depleted) T cell subpopulations. CD8+ T cell depletion (CD4-enriched) did not influence the frequency of IFN-γ, IL-4 and IL-2-secreting cells in mice primed with *tat*/PEG32 or with naked *tat*. In contrast, only IFN-γ-secreting cells were detected in CD8+ purified T cell cultures, although their frequency was significant lower (Fig. 7D and E).

As a whole, these results indicate that the *tat* DNA vaccine elicited long-lasting anti-Tat cellular immune responses, with a mixed Th1–Th2 cytokine profile, thereby confirming the results of previous studies [51,55]. However, the data collected clearly indicate that the presence of the nanoparticles in the vaccine formulation promotes a more efficient priming of both Th1 and Th2 cellular responses, with a prevalence of the Th1-type responses and CTLs.

3.8. Analysis of the humoral response to Tat

ELISA assays were used to detect anti-Tat specific antibodies. After one protein boost, anti-Tat IgG titers were low and only detected in a few mice immunized with *tat*/PEG32 (1022 ± 1769) and with naked DNA (3103 ± 2449) ($p > 0.05$) (Fig. 9A). After a second protein boost, a strong increase of anti-Tat IgG titers was detected in all mice primed with *tat*/PEG32 (mean titers 74191 ± 85967) and with naked *tat* DNA (mean titers 247314 ± 241957) ($p > 0.05$) (Fig. 9B). IgG isotype analysis showed the presence of IgG1 and IgG2a subclasses with similar IgG1/IgG2a ratios of 1.30 and 1.25, respectively, in mice primed with *tat*/PEG32 and with naked *tat*, and a slightly higher prevalence of IgG1 in both groups of mice. The epitope reactivity of the antibodies was mainly directed against the amino-terminal (aa 1–20) and the carboxy-terminal (aa 65–80) regions of Tat in all groups (Table 1). Of note, humoral immune responses were long lasting. In fact, 17 weeks after the second protein boost (week 29) anti-Tat IgG titers were still high in all mice primed with *tat*/PEG32 (mean titers 54899 ± 43141) and with naked *tat* DNA (mean titers 90933 ± 93239) ($p > 0.05$) (Fig. 9C). These results show that *tat*/PEG32 and naked *tat* DNA primed the humoral arm of the immune system, since boosting with the Tat protein and Alum induced strong and long-lasting humoral immunity. In addition, although the difference was not significant ($p > 0.05$), IgG titers were generally higher in mice primed with naked *tat* DNA, thereby suggesting that PEG32 nanoparticles skewed the immune response predominantly towards a Th1-type response.

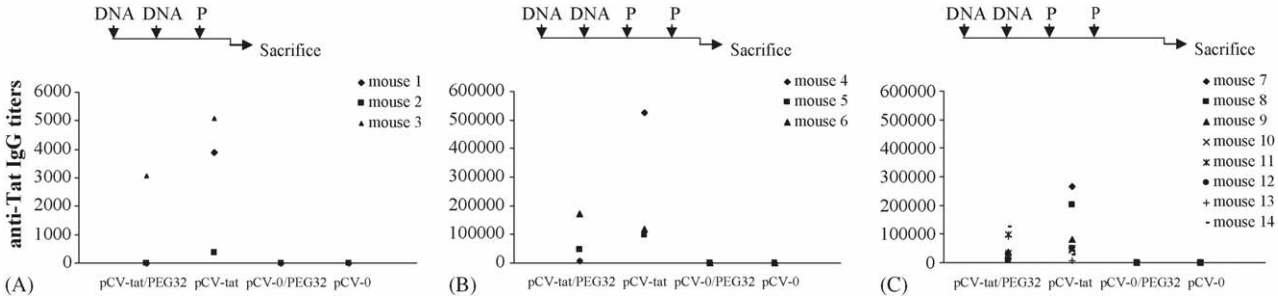

Fig. 9. Anti-Tat IgG responses. Animals were primed i.m. with the DNA/nanoparticle complexes or with naked DNA at weeks 0 and 4, and boosted i.m. with the Tat protein (1 μg) in Alum, or with Alum alone (controls), at weeks 8 (two DNA prime-one protein boost regimen) and at week 12 (two DNA prime-two protein boosts regimen) after the first immunization. Mice were sacrificed at week 10 ($n = 3$) (for the two DNA primes-one protein boost regimen) (A), and at weeks 14 ($n = 3$) (B) and 29 ($n = 8$) (C) (for the two DNA primes-two protein boosts regimen). IgG titers were determined by ELISA. Differences were not statistically significant ($p > 0.05$). The results of one representative experiment out of three are shown.

Table 1
Epitope mapping of anti-Tat IgG[a]

Group	Peptide (aa)							
	1–20	21–40	36–50	46–60	57–72	56–70	65–80	73–86
pCV-*tat*/PEG32 (1 μg/mg)	0.217 ± 0.16	0.011 ± 0	0.008 ± 0	0.008 ± 0	0.001 ± 0	0.009 ± 0	0.111 ± 0.10	0.009 ± 0
pCV-*tat* (1 μg)	0.301 ± 0.23	0.003 ± 0	0.079 ± 0.1	0.022 ± 0	0.007 ± 0	0.007 ± 0	0.110 ± 0.05	0.017 ± 0

[a] Mice were immunized i.m. with pCV-*tat*/PEG32 complexes or with pCV-*tat* DNA alone at weeks 0 and 4, and boosted with Tat protein (1 μg) in Alum at weeks 8 and 12. The results of one representative experiment are shown and correspond to the mean $O.D._{405nm}$ (±S.D.) of mice sacrificed 2 weeks after the second protein boost.

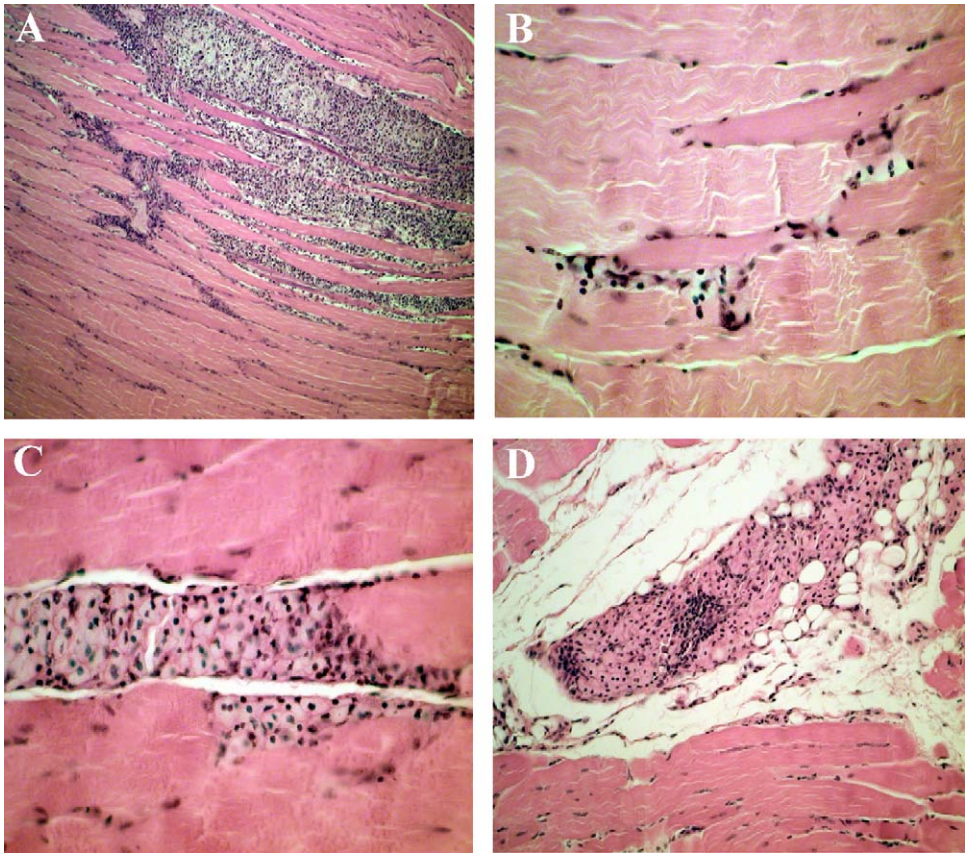

Fig. 10. Histological examination of murine tissues after injection of DNA/PEG32 complexes by the i.m. route. One representative mouse is shown. Inflammatory reaction consisting exclusively of macrophages with clear cytoplasm was quite variable ranging from very conspicuous infiltration among fibers (A) to discrete infiltration around the muscle membrane (B). The muscle fibers show regressive changes and necrosis (C). Inflammatory macrophages infiltration is evident in the adipose tissue surrounding the muscle (D). No differences were reported between mice injected with the DNA/copolymer complexes and naked DNA. Hematoxilyn-Eosin staining: (A and D) 50X; (B) 100X; (C) 250X.

3.9. Safety evaluation

To evaluate the safety of these nanoparticles, the site of injection and the general health of the mice were checked twice a week after immunization. No signs of local or systemic adverse reactions were ever observed in mice receiving the pCV-*tat*/PEG32 or pCV-0/PEG32 complexes, as compared to control mice. At sacrifice, an inflammatory reaction at the site of injection, mainly characterized by infiltration of CD68+ cells, which is a marker of macrophages and dendritic cells, was observed with a similar frequency in mice treated with the pCV-*tat*/PEG32 (87.5%) and pCV-0/PEG32 (85.7%) complexes, and with a slightly lower frequency in mice immunized with naked pCV-*tat* (75%) and pCV-0 DNA (80%), respectively, thus suggesting an adjuvant function of the nanoparticles. As shown in Fig. 10, macrophage infiltration was observed with variable intensity in the interstitial fibroadipose tissue and around the muscle fibers at the site of injection and between the muscle fibers (Fig. 10A). In some cases this infiltration was light and without alterations of the muscle fibers (Fig. 10B), but in others it was associated to their alteration (Fig. 10C). At times the macrophages were observed in the adipose tissue surrounding the injection site only (Fig. 10D). Importantly, no specific alterations that may be related to injection of DNA/nanoparticle complexes were reported in the other organs examined. These results indicate that the nanoparticles are safe and well tolerated in vivo.

4. Discussion

Due to growing concerns regarding the cytotoxicity and immunogenicity of viral DNA delivery systems, the delivery of DNA by means of polymeric systems has become more desirable and advantageous for several reasons such as low toxicity, simplicity of use, ease of large-scale production and lack of specific immune response. In addition, these systems are inexpensive and simple to produce and to store.

Polymeric nano- and micro-particles with encapsulated antigens have become well established in the last decade as potent antigen delivery systems and adjuvants [22,25,26,56]. However, due to the instability/degradation of the bioactive molecule during encapsulation and release [28,29,57], antigen adsorption on the surface of charged nano- and microparticles has very recently been proposed to improve vaccine efficacy.

Modified PLG microparticles carrying antigens on their surface have been developed and shown to be promising delivery systems, as they are able to increase the potency of vaccines in several animal species [17,18,30–32,34,58–61]. Potent immune responses were also obtained after immunization with antigens adsorbed onto PLA lamellar substrate microparticles [18]. Moreover, antigen-coated wax nanoparticles were recently shown to be more immunogenic than Alum and lipid A formulations containing the same antigen [58]. Although these systems have been used successfully, a common feature of the described nanoparticles is the use of surfactants and/or detergents required during particle preparation for the generation of surface functional groups. However, these surfactants/detergents may often interfere with the reproducibility of particle size and size distribution, and of the vaccine formulation, and may affect the biocompatibility and pharmacokinetic behaviour of the nanoparticles [12,62].

For the rational development of improved DNA vaccine delivery systems, in this study new cationic polymeric nanoparticles for reversible adsorption of native DNA at their surface were synthesized by emulsion polymerization and characterized in vitro and in vivo. These particles possess an innovative structure characterized by the presence of functional groups covalently bound to the particle surface. This structure represents an advantage as compared to previously described nanoparticles since it increases the stability and reproducibility of the vaccine formulation and avoids physical desorption and/or instability/toxicity effects associated with the use of free surfactants and/or detergents simply adsorbed on their surface. In particular, these functional nanoparticles are obtained by controlled polymerization of the single acrylic monomers in water and not by surface functionalization or chemical conjugation of cationic polymers to the preformed particles, as recently described by Kasturi et al. [63].

Our results indicate that emulsion polymerization leads to the formation of highly hydrophilic outer shell which allows adsorption of high doses of DNA. The binding is reversible and occurs mainly through electrostatic interactions between the cationic surface of the nanoparticles and the negatively charged DNA molecules, as suggested by the observation that DNA binding is abolished in the presence of 1 M NaCl and that 80% of the loaded DNA is promptly released from the nanoparticle surface in the presence of 1 M NaCl. Of note, the binding and release processes did not affect the physical structure of the DNA, thus indicating that adsorption/desorption processes do not affect DNA integrity.

The results show that these nanoparticles are not toxic for the cells even at very high doses (10 mg/ml) and, most importantly, that they are safe in vivo. In fact, neither local adverse reactions nor differences in the health and behaviour were observed in mice vaccinated with DNA/nanoparticle complexes or with naked pCV-*tat* or pCV-0 DNA. Moreover, no specific histological alterations that may be related to the injection of the complexes were observed, as indicated by similar histological pictures reported for all mice. In this respect, it should be noted that polymers were chosen based on their biocompatibility. Indeed, PMMA has been used in surgery for over 50 years and PMMA-based particles have already been shown to be very promising as adjuvants for vaccines and to be slowly biodegradable [35,64], and PEG is a non-toxic, water-soluble polymer with proven biocompatibility.

The DNA/nanoparticle complexes are taken up by the cells where the DNA is released and expressed. Indeed, expression of the luciferase gene was detected only with the DNA/PEG32 samples, freshly prepared or stored in powder-form at room temperature for several weeks, as compared to cells incubated with a similar dose of naked DNA, thereby demonstrating that the nanoparticles increased the stability and the shelf-life of the DNA vaccine. A possible explanation for this effect is that the nanoparticles, in addition to favouring cellular uptake of DNA, protect it from enzymatic degradation and exert a depot effect, as also suggested by the results of the mice studies.

To evaluate the immunogenicity of novel DNA/PEG32 vaccine formulations and adjuvanticity of the nanoparticles, we chose the HIV-1 *tat* gene as model vaccine relevant antigen [36,37]. Previous studies have shown that HIV-1 Tat is immunogenic in mice, monkeys and humans and, in particular, in the form of naked plasmid DNA it induces mainly cellular immune responses, whereas in the form of native protein Tat elicits broad humoral and cellular responses [36,37]. In addition, the Tat-vaccine has recently completed preventive and therapeutic phase I clinical testing in Italy and, based on the results, has being granted for funding for phase II-proof of concept trial as both preventive and therapeutic vaccine. Finally, due to its immunomodulatory properties ([52], Gavioli et al., unpublished data), Tat will soon be tested in humans in combination with Env.

Of note, several studies have shown that vaccination with naked *tat* DNA, using high doses of different *tat* expressing plasmids and multiple boosts, is immunogenic in rodents, non-human primates and humans [36,37]. In particular, in these studies plain vaccination with naked *tat* DNA elicited predominant cellular immune responses and very low or absent antibody titers and, interestingly, anti-Tat CTLs were detected only in few of these studies [3,51,55,65–68]. In our monkey study, 0.5–1 mg of pCV-*tat* DNA was given intramuscularly for seven immunizations [68]. Another study [67] showed induction of antigen-specific CTL responses in mice immunized six times with 6 μg of a different *tat* expressing plasmid by gene gun. In the same study anti-Tat CTL responses, however, were not detected in mice immunized six times i.m. with 150 μg of *tat* DNA. Finally, it has recently been shown that mice vaccinated 2–4 times i.m. with a codon-optimized *tat* gene developed higher anti-Tat CTL activities as compared to immunization with wild-type DNA [51]. In this context, we have also shown that addition of a polymeric delivery system, such as cationic block copolymers, to the pCV-*tat* DNA vaccine strongly enhances Tat-specific CTL responses in mice after six i.m. immunizations in the absence, however, of detectable antibody responses [47]. Since several pieces of experimental evidence indicate the existence of an inverse correlation between humoral and cellular immune responses to Tat and disease onset, and as a broader immunity is generally a better correlate of protection against infectious diseases and tumors, in the present study we decided to adopt a DNA prime-protein boost protocol to determine whether the combination of PEG32 nanoparticles and the prime-boost vaccination regimen may broaden the type of immunity against this DNA vaccine antigen.

The results demonstrate that the *tat*/PEG32-based vaccine, containing a very low amount of DNA (1 μg), primed both humoral and cellular immune responses with a mixed Th1–Th2 profile, in a fashion similar to naked *tat* DNA. These responses were long-lasting and mainly sustained by the presence of CD4+ T memory cells. However, in mice primed with the *tat*/PEG32 vaccine cellular immune responses were induced more efficiently as compared to mice primed with the naked DNA. This is suggested by the presence of a significant increase of CD4+ T cell proliferation and higher number of IFN-γ, IL-4 and IL-2 secreting cells after two DNA/PEG32 inoculations and one boost with the Tat protein and Alum, and by the presence of significantly higher numbers of IFN-γ producing cells and CTLs after two DNA/PEG32 primes and two protein boosts. In addition, the results show that IgG titers were generally lower in *tat*/PEG32-primed mice as compared to naked DNA-primed animals, both after one and two protein boosts. The data thus suggest that the presence of the nanoparticles in the DNA vaccine formulation predominantly skewed the immune response toward a Th1-type profile and enhanced antigen-specific CTL responses. In addition, the results indicate that at least one protein boost is required to raise significant antibody titers after priming with *tat* DNA, either naked or formulated with the nanoparticles. Nevertheless, the results do not rule out the possibility that the described new nanoparticles may be of potential use as well for the development of plain DNA vaccines, and to test this hypothesis experiments are ongoing using higher doses of the DNA vaccine antigen and different antigens.

In conclusion, the results indicate that these novel cationic nanoparticles represent a very promising approach in gene delivery for vaccination purposes. They are safe, inexpensive, easy to produce and to store, and are able to increase the stability of the DNA vaccine. The two components of the complexes can be mixed at room temperature without any purification steps, and they can also be stored at room temperature in powder form without a cold chain requirement. They allow the use of a low amount of DNA and few immunization boosts. Finally, they efficiently prime both arms of the immune system and enhance the antigen-specific Th1 responses and CTLs.

Acknowledgements

This work was supported by grants from the Italian Concerted Action on HIV-AIDS Vaccine Development (ICAV) and from MURST 40%. We are grateful to M. Magnani (Diatheva, Fano, Italy) for providing the Tat protein, to R. De Michele and M. Scarletti (University of Ferrara) for excellent technical work and animal care, and to R. Guerrini (UFPeptide, s.r.l., Ferrara) for synthesis of the Tat peptide.

References

[1] Gurunathan S, Wu CY, Seder RA. DNA vaccines: a key for inducing long-term cellular immunity. Curr Opin Immunol 2000;12:442–7.

[2] Donnelly JJ, Wahren B, Liu MA. DNA vaccines: progress and challenges. J Immunol 2005;175:633–9.

[3] Calarota S, Bratt G, Nordlund S, Hinkula J, Leandersson AC, Sandstrom E, et al. Cellular cytotoxic response induced by DNA vaccination in HIV-1-infected patients. Lancet 1998;351:1320–5.

[4] Wang R, Doolan DL, Le TP, Hedstrom RC, Coonan KM, Charoenvit Y, et al. Induction of antigen-specific cytotoxic T lymphocytes in humans by a malaria DNA vaccine. Science 1998;282:476–80.

[5] Chen WC, Huang L. Non-viral vector as vaccine carrier. Adv Gen 2005;54:315–37.

[6] Crommelin DJA, Daemen T, Scherphof G, Vingerhoeds MH, Heeremans JLM, Kluft C, et al. Liposomes: vehicles for the targeted and controlled delivery of peptides and proteins. J Control Release 1997;46:165–75.

[7] Nugent J, Wan Po L, Scott E. Design and delivery of non-parental vaccines. J Clin Pharm Ther 1998;23:257–85.

[8] Thierry AR, Rabinovich P, Peng B, Mahan LC, Bryant JL, Gallo RC. Characterization of liposome-mediated gene delivery. Expression, stability and pharmacokinetics of plasmid DNA. Gene Ther 1997;4:226–37.

[9] O'Hagan DT, Singh M, Ulmer JB. Microparticles for the delivery of DNA vaccines. Immunol Rev 2004;199:191–200.

[10] Majeti NV, Kumar R. Nano and microparticles as controlled drug delivery devices. J Pharm Sci 2000;3:234–58.

[11] Alpar HO, Papanicolaou I, Bramwell VW. Strategies for DNA vaccine delivery. Expert Opin Drug Deliv 2005;2:829–42.

[12] Rihova B. Biocompatibility of biomaterials: hemocompatibility, immunocompatibility and biocompatibility of solid polymeric materials and soluble targetable polymeric carriers. Adv Drug Deliv Rev 1996;21:157–76.

[13] Cui Z, Mumper RJ. Genetic immunization using nanoparticles engineered from microemulsion precursors. Pharm Res 2002;19:939–46.

[14] Cui Z, Mumper RJ. Topical immunization using nanoengineered genetic vaccines. J Control Release 2002;81:173–84.

[15] Cui Z, Mumper RJ. Intranasal administration of plasmid DNA-coated nanoparticles results in enhanced immune responses. J Pharm Pharmacol 2002;54:1195–203.

[16] Oster CG, Kim N, Grode L, Barbu-Tudoran L, Schaper AK, Kaufmann SH, et al. Cationic microparticles consisting of poly(lactide-co-glycolide) and polyethylenimine as carriers systems for parental DNA vaccination. J Control Release 2005;104:359–77.

[17] Mollenkopf HJ, Dietrich G, Fensterle J, Grode L, Diehl KD, Knapp B, et al. Enhanced protective efficacy of a tuberculosis DNA vaccine by adsorption onto cationic PLG microparticles. Vaccine 2004;22:2690–5.

[18] Jabbal-Gill I, Lin W, Jenkins P, Jimenez M, Illum L, Davis SS, et al. Potential of polymeric lamellar substrate particles (PLSP) as adjuvants for vaccines. Vaccine 1999;18:238–50.

[19] Men Y, Thomasin C, Merkle H, Gander B. A single administration of tetanus toxoid in biodegradable microspheres elicit T cell and antibody responses similar or superior to those obtained with aluminium hydroxide. Vaccine 1995;13:683–9.

[20] Anderson JM, Shive MS. Biodegradation and biocompatibility of PLA and PLGA microspheres. Adv Drug Deliv Rev 1997;28:5–24.

[21] Eldridge JH, Staas JK, Meulbroek JA, Tice TR, Gilley RM. Biodegradable and biocompatible poly(D, L-lactide-co-glycolide) microspheres as an adjuvant for staphylococcal enterotoxin B toxoid which enhances the level of toxin-neutralizing antibodies. Infect Immun 1991;59:2978–86.

[22] Johansen P, Men Y, Merkle HP, Gander B. Revisiting PLA/PLGA microspheres: an analysis of their potential in parenteral vaccination. Eur J Pharm Biopharm 2000;50:129–46.

[23] O'Hagan DT. Recent advances in vaccine adjuvants for systemic and mucosal administration. J Pharm Pharmacol 1998;59:1–10.

[24] O'Hagan DT. Recent developments in vaccine delivery systems. Curr Drug Targets Infect Disord 2001;1:273–86.

[25] O'Hagan DT, Jeffery H, Davis SS. Long-term antibody responses in mice following subcutaneous immunization with ovalbumin entrapped in biodegradable microparticles. Vaccine 1993;11:965–9.

[26] O'Hagan DT, Rahman D, McGee JP, Jeffery H, Davies MC, Williams P, et al. Biodegradable microparticles as controlled release antigen delivery systems. Immunology 1991;73:239–42.

[27] Nedrud JG, Lamm ME. Adjuvants and the mucosal immune system. In: Spriggs DR, Koff WC, editors. Topics in vaccine adjuvant research. Boca Raton: CRC; 1991. p. 51–67.

[28] Singh M, Chesko J, Kazzaz J, Ugozzoli M, Kan E, Srivastava I, et al. Adsorption of a novel recombinant glycoprotein from HIV (Env gp120dV2 SF162) to anionic PLG microparticles retains the structural integrity of the protein, whereas encapsulation in PLG microparticles does not. Pharm Res 2004;21:2148–52.

[29] Kim JH, Taluja A, Knutson K, Han Bae Y. Stability of bovine serum albumin complexed with PEG-poly(l-histidine) diblock copolymer in PLGA microspheres. J Control Release 2005;109:86–100.

[30] O'Hagan D, Singh M, Ugozzoli M, Wild C, Barnett S, Chen M, et al. Induction of potent immune responses by cationic microparticles with adsorbed human immunodeficiency virus DNA vaccines. J Virol 2001;75:9037–43.

[31] Xie H, Gursel I, Ivins BE, Singh M, O'Hagan DT, Ulmer JB, et al. CpG oligodeoxynucleotides adsorbed onto polylactide-co-glycolide microparticles improve the immunogenicity and protective activity of the licensed anthrax vaccine. Infect Immun 2005;73:828–33.

[32] O'Hagan DT, Singh M, Dong C, Ugozzoli M, Berger K, Glazer E, et al. Cationic microparticles are a potent delivery system for a HCV DNA vaccine. Vaccine 2004;23:672–80.

[33] Singh M, Kazzaz J, Ugozzoli M, Chesko J, O'Hagan DT. Charged polylactide co-glycolide microparticles as antigen delivery systems. Expert Opin Biol Ther 2004;4:483–91.

[34] Singh M, Kazzaz J, Chesko J, Soenawan E, Ugozzoli M, Giuliani M, et al. Anionic microparticles are a potent delivery system for recombinant antigens from Neisseria meningitidis serotype B. J Pharm Sci 2004;93:273–82.

[35] Stieneker F, Kreuter J, Lower J. High antibody titers in mice with polymethylmethacrylate nanoparticles as adjuvant for HIV vaccines. AIDS 1991;5:431–5.

[36] Caputo A, Gavioli R, Ensoli B. Recent advances in the development of HIV-1 Tat-based vaccines. Curr HIV Res 2004;2:357–76.

[37] Ferrantelli F, Cafaro A, Ensoli B. Nonstructural HIV proteins as targets for prophylactic or therapeutic vaccines. Curr Opin Biotechnol 2004;15:543–56.

[38] Sparnacci K, Tondelli L, Laus M. Core shell functional nanospheres for oligonucleotide delivery. III. Stealth nanospheres. J Polym Sci, Polym Chem 2000;38:3347–54.

[39] Rolland A, Gibassier D, Sado P, Le Verge R. Purification and physicochemical properties of polyacrylic nanoparticles. J Pharm Belg 1986;41:94–105.

[40] Laus M, Sparnacci K, Lelli M, Vannini R, Tondelli L. Core-shell functional nanospheres for oligonucleotide delivery. II. J Polym Sci A: Polym Chem 2000;38:1110–7.

[41] Sparnacci K, Laus M, Tondelli L, Bernardi C, Magnani L, Corticelli F, et al. Core-shell microparticles by dispersion polymerization as promising delivery systems for proteins. J Biomater Sci Polym Edn 2005;16:1557–74.

[42] Okubo M, Yamamoto Y, Kamei S. Studies on suspension and emulsion. 58. Xps analysis (esca) of the surface-composition of poly(styrene 2-hydroxyethyl methacrylate) microspheres produced by emulsifier-free emulsion polymerization. Colloid Polym Sci 1989;267:861–5.

[43] Arya SK, Guo C, Joseph SF, Wong-Staal F. The *trans*-activator gene of human T-lymphotropic virus type III (HTLV-III). Science 1985;229:69–73.
[44] Wright CM, Felber BK, Paskalis H, Pavlakis GN. Expression and characterization of the *trans*-activator of HTLV-III/LAV virus. Science 1986;234:988–92.
[45] Caputo A, Sodroski JG, Haseltine WA. Constitutive expression of HIV-1 tat protein in human Jurkat T cells using a BK virus vector. J Acquir Immune Defic Syndr 1990;3:372–9.
[46] Mosmann T. Rapid colorimetric assay for cellular growth and survival: application to proliferation and cytotoxicity assays. J Immunol Methods 1983;65:55–63.
[47] Caputo A, Gavioli R, Altavilla G, Brocca-Cofano E, Boarini C, Betti M, et al. Immunization with low doses of HIV-1 tat DNA delivered by novel cationic block copolymers induces CTL responses against Tat. Vaccine 2003;21:1103–11.
[48] Ensoli B, Buonaguro L, Barillari G, Fiorelli V, Gendelman R, Morgan RA, et al. Release, uptake, and effects of extracellular human immunodeficiency virus type 1 Tat protein on cell growth and viral transactivation. J Virol 1993;67:277–87.
[49] Chang HC, Samaniego F, Nair BC, Buonaguro L, Ensoli B. HIV-1 Tat protein exits from cells via a leaderless secretory pathway and binds to extracellular matrix-associated heparan sulfate proteoglycans through its basic region. AIDS 1997;11:1421–31.
[50] Fanales-Belasio E, Moretti S, Nappi F, Barillari G, Micheletti F, Cafaro A, et al. Native HIV-1 Tat protein targets monocyte-derived dendritic cells and enhances their maturation, function, and antigen-specific T cell responses. J Immunol 2002;168:197–206.
[51] Ramakrishna L, Anand KK, Mohankumar KM, Ranga U. Codon optimization of the tat antigen of human immunodeficiency virus type 1 generates strong immune responses in mice following genetic immunization. J Virol 2004;78:9174–89.
[52] Gavioli R, Gallerani E, Fortini C, Fabris M, Bottoni A, Canella A, et al. HIV-1 tat protein modulates the generation of cytotoxic T cell epitopes by modifying proteasome composition and enzymatic activity. J Immunol 2004;173:3838–43.
[53] Caputo A, Brocca-Cofano E, Castaldello A, De Michele R, Altavilla G, Marchisio M, et al. Novel biocompatible anionic polymeric microspheres for the delivery of the HIV-1 Tat protein for vaccine application. Vaccine 2004;22:2910–24.
[54] Sokak RR, Rohlf FJ. Estimation and hypothesis testing. In: Sokak RR, Rohlf F, editors. Biometry: the principles and practice of statistics in biological research. San Francisco: Freeman; 1981. p. 128–35.
[55] Caselli E, Betti M, Grossi MP, Balboni PG, Rossi C, Boarini C, et al. DNA immunization with HIV-1 tat mutated in the transactivation domain induces humoral and cellular immune response against wild-type Tat. J Immunol 1999;162:5631–8.
[56] Jilek S, Merkle HP, Walter E. DNA-loaded biodegradable microparticles as vaccine delivery systems and their interaction with dendritic cells. Adv Drug Deliv Rev 2005;57:377–90.
[57] Gupta RK, Chang AC, Siber GR. Biodegradable polymer microspheres as vaccine adjuvants and delivery systems. Dev Biol Stand 1998;92:63–78.
[58] Cui Z, Patel J, Tuzova M, Ray P, Phillips R, Woodward JG, et al. Strong T cell type-1 immune responses to HIV-1 Tat (1–72) protein-coated nanoparticles. Vaccine 2004;22:2631–40.
[59] Kaur R, Rauthan M, Vrati S. Immunogenicity of a cationic microparticle-adsorbed plasmid DNA encoding Japanase encephalistis virus envelope protein. Vaccine 2004;22:2776–82.
[60] Otten G, Schaefer M, Greer C, Calderon-Cacia M, Coit D, Kazzaz J, et al. Induction of broad and potent anti-human immunodeficiency virus immune responses in rhesus macaques by priming with a DNA vaccine and boosting with protein-adsorbed polylactide coglycolide microparticles. J Virol 2003;77:6087–92.
[61] Denis-Mize KS, Dupuis M, Singh M, Woo C, Ugozzoli M, O'Hagan DT, et al. Mechanisms of increased immunogenicity for DNA-based vaccines adsorbed onto cationic microparticles. Cell Immunol 2003;225:12–20.
[62] Lode J, Fichtner I, Kreuter J, Berndt A, Diederichs JE, Reszka R. Influence of surface-modifying surfactants on the pharmacokinetic behavior of ^{14}C-poly(methylmethacrylate) nanoparticles in experimental tumor models. Pharm Res 2001;18:1613–9.
[63] Kasturi SP, Sachaphibulkij K, Roy K. Covalent conjugation of polyethyleneimine on biodegradable microparticles for delivery of plasmid DNA vaccines. Biomaterials 2005;26:6375–85.
[64] Kreuter J, Speiser PP. New adjvants on a polymethylmethacrylate base. Infect Immunol 1976;13:204–10.
[65] Hinkula J, Svanholm C, Schawartz S, Lundholm P, Brytting M, Engstrom G, et al. Recognition of prominent viral epitopes induced by immunization with human immunodeficiency virus type 1 regulatory genes. J Virol 1997;71:5528–39.
[66] Hinkula J, Lundholm P, Wahren B. Nucleic acid vaccination with HIV regulatory genes: a combination of HIV-1 genes in separate plasmids induces strong immune responses. Vaccine 1997;15:874–8.
[67] Tahtinem M, Strengell M, Collings A, Pitkanen J, Kjerrstrom A, Hakkarainen K, et al. DNA vaccination in mice using HIV-1 nef, rev and tat genes in self-replicating pBN-vector. Vaccine 2001;19:2039–47.
[68] Cafaro A, Titti F, Fracasso C, Maggiorella MT, Baroncelli S, Caputo A, et al. Vaccination with DNA containing tat coding sequences and unmethylated CpG motifs protects cynomolgus monkeys upon infection with simian/human immunodeficiency virus (SHIV89.6P). Vaccine 2001;19:2862–77.